Journal of Nano- and Electronic Physics
Vol. **8** No 2, 02034(8pp) (2016)

Журнал нано- та електронної фізики
Том **8** № 2, 02034(8cc) (2016)

Diffraction Radiation Oscillator with Asymmetric Open Resonant System. Part 2. Hot Test Results of Diffraction Radiation Oscillator

V.S. Miroshnichenko*, I.O. Kovalov

O.Ya. Usikov Institute for Radiophysics and Electronics NAS of Ukraine
12, Akad. Proskury St., 61085 Kharkiv, Ukraine

(Received 04 April 2016; revised manuscript received 09 June 2016; published online 21 June 2016)

The hot test results of diffraction radiation oscillator with asymmetric open resonant system, in which the periodic structure was shifted to the field spot periphery of the operating TEM_{00q}-mode, are presented. It is shown, that displacement of the periodic structure, in double grating form, to field spot periphery of TEM_{00q}-mode allows extending the single-mode frequency tuning range and improves the overall efficiency of diffraction radiation oscillator. The mode competition features in diffraction radiation oscillator with double grating and asymmetric open resonant system are considered. The investigations were carried out in 8-mm waveband.

Keywords: Diffraction radiation oscillator, Open resonant system, Periodic structure, Double grating, Millimeter waves.

DOI: 10.21272/jnep.8(2).02034 PACS numbers: 84.40.Fe, 85.40. – x, 42.82Bg

1. INTRODUCTION

Diffraction radiation oscillator (DRO) with periodic structure in double grating form has more higher level of output power and efficiency due to effective using of the ribbon electron beam on its thickness [1, 2]. The significant disadvantage such DRO is relatively narrow frequency tuning range, as a result of the strong double grating influence on resonant field of operating TEM_{00q}-mode into its open resonant system (ORS). To extend DRO frequency tuning range we suggest using of asymmetric ORS, in which the double grating is displaced from longitudinal axis of the system to field spot periphery of operating TEM_{00q}-mode. In the first part of present paper [3] the cold test results of resonant modes properties, exciting in the asymmetric ORS with double grating, were shown. It was established, that the double grating shifting to field spot periphery reduces its influence on resonant field of operating TEM_{00q}-mode and decreases ohmic loss in the grating, that contributes to increase of ORS Q-factor and to expand of single-mode frequency tuning range.

In the present paper the hot test results of the DRO-model with asymmetric ORS are presented. The mirrors parameters and the optimal displacement of double grating from resonator longitudinal axis were used according to the cold test results of the resonant modes properties in asymmetric ORS [3]. In order to estimate the advantages of DRO with the asymmetric ORS, the measurements of output characteristics of the DRO-model were carried out in parallel for symmetric and asymmetric location of the double grating in the field spot of operating TEM_{00q}-mode. For the DRO-model with asymmetric and symmetric ORS a comparison of following output parameters were conducted: single-mode frequency tuning range, oscillations starting current, output power level and overall efficiency of the oscillator. Also in the present paper the feautures of modes competition in DRO-model with symmetric and asymmetric ORS were analyzed. The investigations were carried out in 8-mm waveband.

2. DISMOUNTABLE DRO-MODEL AND HOT TEST EQUIPMENT

For experimental investigations the dismountable model of DRO with symmetric and asymmetric ORS, operating under continuous vacuum pumping, was used (Fig. 1). The DRO-model included: cylindrical vacuum chamber 1 with inner diameter ∅80 mm; moving spherical mirror unit 2; flat mirror unit 3 with a double grating 4 and electron gun 5. The cylindrical grooves with vacuum rubber at the each mirror units provided coincidence of the longitudinal ORS axis with the vacuum chamber axis. The electron gun formed ribbon electron beam with cross-section 0.12×3.8 mm^2, which was passed in the double grating channel of width 0.30 mm. The electron beam axis was placed at the double grating half-height. The one side of double grating was leveled to the flat mirror surface. The external electromagnet 7 provided focused magnetic field with strength $B = 0.5$ T. The interception of electron beam by double grating was controlled by isolated collector 8. The flat mirror unit 3 allowed symmetric placement of the double grating relative to ORS axis, and also its shifted location along *OX* axis to field spot periphery of TEM_{00q}-mode.

The measurements of output parameters had been carried out at pulsed operation, that allowed to decrease thermal heating of DRO-model in ~ 4 times. The accelerating voltage pulses with controlled amplitude (2.5 ÷ 4.0) kV and repetition frequency 50 Hz were fed by power supply without ripple filter. The oscillation pulse length was ~ 2 ms at duty cycle ~ 10 %, that allowed direct measurements of output power by wattmeter with the thermoelectric transducer ($P_{max} \leq 10$ W). The oscillation frequency of DRO-model had been controlled by the resonance wavemeter (Fig. 2).

* mirosh@ire.kharkov.ua

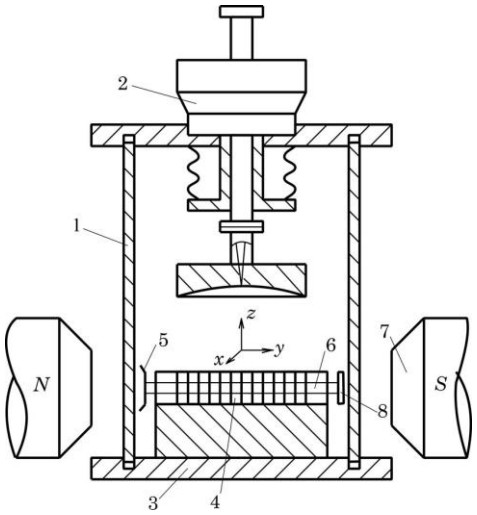

Fig. 1 – The schematic of the dismountable DRO-model, operating under continuous vacuum pumping: 1 – cylindrical chamber; 2 – moving spherical mirror unit; 3 – flat mirror unit; 4 – double grating; 5 – electron gun; 6 – ribbon electron beam; 7 – electromagnet; 8 – isolated collector

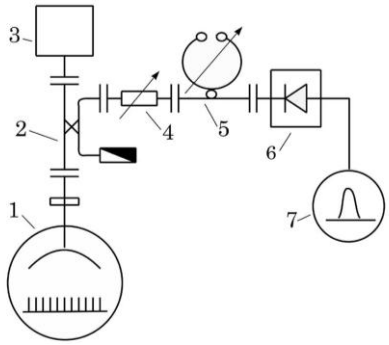

Fig. 2 – The schematic of hot test equipment for the DRO-model: 1 – dismountable DRO-model; 2 – directional coupler (– 30 dB); 3 – wattmeter; 4 – adjustable attenuator; 5 – resonance wavemeter; 6 – detector section; 7 – oscilloscope

The TEM_{00q}-mode identification, excited in DRO by electron beam at oscillation frequency f, was made on accelerating voltage amplitude U_a, which satisfies the synchronism of electron beam velocity v_e with phase velocity v_{ph} for 1-st space harmonic of the double grating field:

$$v_e = v_{ph} = c\frac{l}{\lambda} = 5{,}93 \cdot 10^5 \sqrt{U_{ph}[\text{Volt}]}, \qquad (1)$$

where c is the speed of light, l is the grating period, λ is free-space wavelength. Also, for the TEM_{00q}-mode identification we took into account the resonant distance between mirrors $D_{00q}(f)$, which was defined at the cold test of ORS parameters [3]. Note, that for the TEM_{00q}-mode we assumed that longitudinal index q describes only the number of resonant field variation along OZ in the intermirror space, as in OR with smooth mirrors. For the higher TEM_{mnq}-modes the transversal indexes m, n describe the number of field variation along OX and OZ axis (Fig. 1).

Let's designate as f_π – the frequency for complete matching of "half-wave" double grating with resonant field:

$$f_\pi = \frac{c}{2b}\sqrt{1+\left(\frac{2b}{\lambda_{cr}}\right)^2}, \qquad (2)$$

where b is the double grating height along OZ axis (Fig. 1), λ_{cr} is a critical wavelength of the H_{10}-mode in the elementary waveguide, formed by opposite slots of double grating [3]. At frequency f_π the resonant distances $D_{mnq}(f)$ for TEM_{mnq}-modes can be defined from the resonant condition in semispherical OR with smooth mirrors:

$$\frac{2D_{mnq}}{\lambda_\pi} = q + \frac{1}{2\pi}(1+m+n)\arccos\left(1-\frac{2D_{mnq}}{R_{sph}}\right). \qquad (3)$$

Initially, in the experiment, to make a correct properties comparison of DRO-model with symmetric and asymmetric ORS, the double grating was placed symmetric to longitudinal ORS axis (OZ axis), and then it was displaced along OX axis to the optimal distance $\xi = 6.0$ mm [3]. The used mirrors in DRO-model had the same parameters, as it was at the cold test of ORS [3]: the spherical mirror had curvature radius $R_{sph} = 50$ mm and diameter ∅55 mm; the flat mirror with double grating had diameter ∅58 mm and was symmetrically truncated on two sides to 32 mm to allocate electron gun and collector in DRO-model.

3. DRO-MODEL WITH DOUBLE GRATING OF HEIGHT $B = 8.0$ MM

The possibility of extending the single-mode frequency tuning range at significant growth of ORS Q-factor was shown by the cold test of resonant modes properties in asymmetric ORS with a double grating. However, many additional factors influence on the output parameters of DRO. So, just carrying out the hot test of DRO with the asymmetric ORS by oscillations operation allows us to estimate the advantage of its using in DRO-modifications.

The oscillation starting current and output power level of DRO througout frequency tuning range were determined at hot test. The loaded Q-factor and the coupling coefficient of ORS on operating TEM_{00q}-mode were defined at cold test [3]. In DRO-model we used the double grating with length $L = 25$ mm, grating period $l = 1.00$ mm, slots width $d = 0.50$ mm, and slots depth $h = 2.56$ mm. The double grating height along longitudinal ORS axis was $b = 8.0$ mm (OZ axis on Fig. 1). The selected parameters of double grating provide the complete phase matching with resonant field at frequency $f_\pi = 33.7$ GHz.

The investigations of DRO output power level along the frequency tuning range were measured at electron beam current $I_a = 120$ mA. The output power maximum on the operating TEM_{004}-mode in DRO with the symmetric ORS was observed on frequencies near $f_\pi = 33.7$ GHz, and was $P_{max} = 39$ W. The frequency tuning range at the output power level $P \geq 0.5\,P_{max}$ was $\Delta f/f_\pi = 6.3$ %. In DRO with the asymmetric ORS, when the double grating was shifted on $\xi = 6.0$ mm, the output power maximum on the operating TEM_{004}-mode was observed on frequency $f = 32.8$ GHz and was

P_{max} = 34 W. The frequency tuning range extended to low-frequency region and was: $\Delta f/f_\pi$ = 9.4% (Fig. 3a). The oscillation starting current in DRO with the asymmetric ORS increased in 1.5 ÷ 2 times in comparison with starting current in DRO with symmetric placement of double grating and was I_{st} = (45÷60) mA at frequencies near f_π (Fig. 3b).

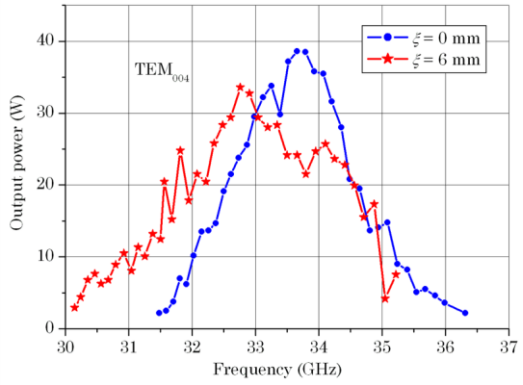

a

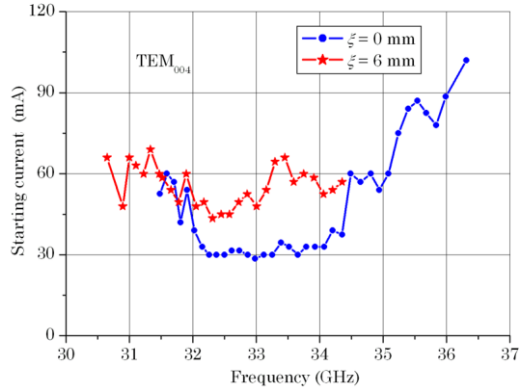

b

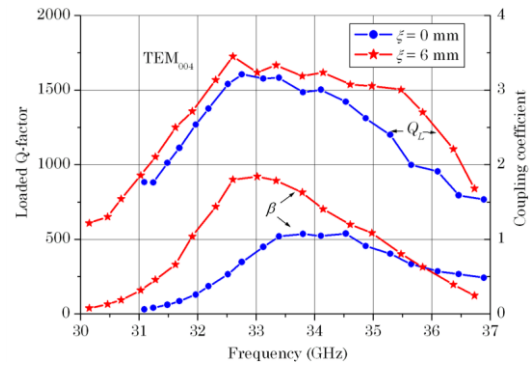

c

Fig. 3 – The characteristics of DRO-model with symmetric and asymmetric ORS at operation on TEM_{004}-mode

The increase of loaded Q-factor in asymmetric ORS on TEM_{004}-mode was not significant (Fig. 3c), therefore the starting current growth probably due to resonant field amplitude decrease in double grating by its displacement to field spot periphery of TEM_{004}-mode. In the same time, the significant growth of coupling coefficient β in asymmetric ORS (Fig. 3c) promoted the growth of overall efficiency of DRO and the growth of output power level at low-frequency region.

The resonant effect of the radiation loss on the frequency tuning range was more clearly demonstrated, when DRO operated on TEM_{006}-mode. Thus, the maximal output power of DRO was observed near f_π independently from the type of used ORS and was P_{max} = 34 W (Fig. 4a). In DRO with asymmetric ORS, the frequency tuning range extended to $\Delta f/f_\pi$ = 8.5 % and the drops of the output power reduced at frequency tuning.

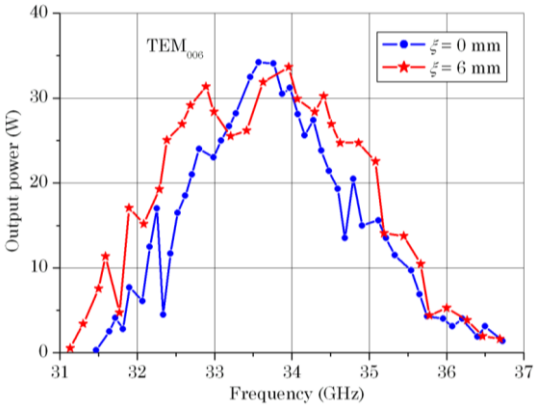

a

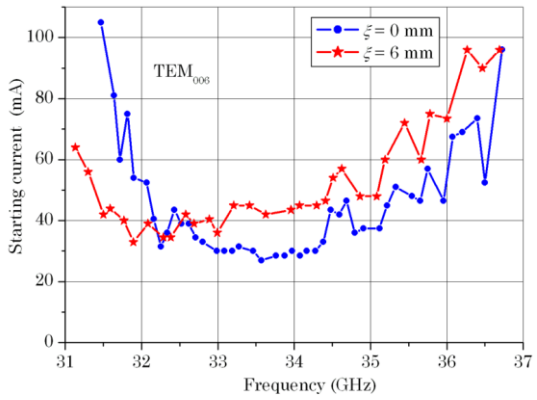

b

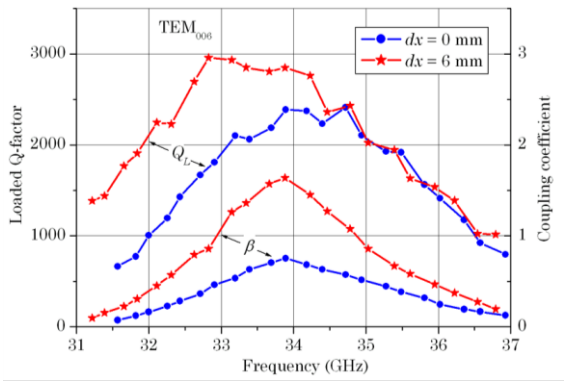

c

Fig. 4 – The characteristics of the DRO-model with symmetric and asymmetric ORS at operation on TEM_{006}-mode

The oscillation starting current in DRO with asymmetric ORS growth not more than in 1.5 times (Fig. 4b) and on frequencies near f_π was I_{st} = (41÷44) mA. Here, the increasing of loaded Q-factor in asymmetric ORS plays an essential role (Fig. 4c). The coupling coefficient

of asymmetric ORS reached the maximum $\beta = 1.6$ on frequencies near f_π.

A comparison of the beam-field interaction efficiency in DRO with symmetric and asymmetric ORS had been carried out on frequencies near f_π,, where DRO had maximal output power throughout frequency tuning range. The first investigations of efficiency on beam-field interaction were realized in DRO with double grating length $L = 25$ mm $\approx 3w_{0y}$ (w_{0y} is the field spot radius on flat mirror along OY axis). For DRO-operation on TEM_{006}-mode the linear growth of output power at beam current increase was observed in DRO with symmetric and asymmetric ORS (Fig. 5a). The overall efficiency N in DRO with symmetric ORS reached saturation $N_{max} = 8.4$ % at beam current $I_a \geq 120$ mA. In DRO with asymmetric ORS overall efficiency reached saturation $N_{max} = 7.9$ % at beam current $I_a \geq 140$ mA.

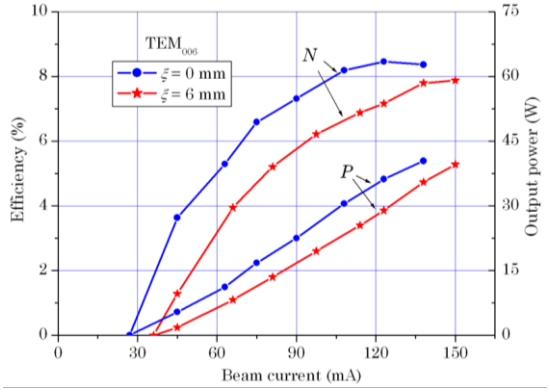

a

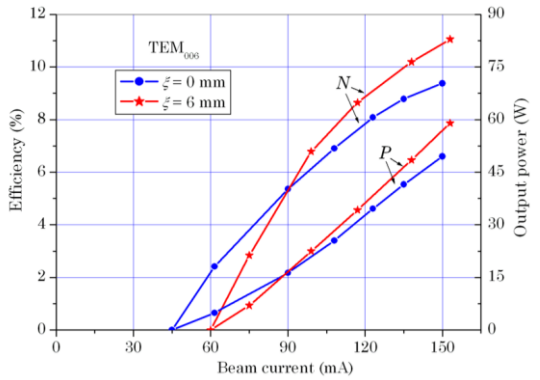

b

Fig. 5 – The efficiency and output power of DRO with symmetric ORS and asymmetric ORS for double grating length $L = 25$ mm (a) and $L = 17$ mm (b)

When we shortened the double grating length to $L = 17$ mm $\approx 2w_{0y}$ the saturation of overall efficiency wasn't observed up to beam current $I_a = 150$ mA both in DRO with symmetric ORS and with asymmetric ORS (Fig. 5b). In DRO with asymmetric ORS at beam current $I_a > 90$ mA the output power and overall efficiency of DRO exceeded the same parameters for DRO with symmetric ORS. The maximal output power and overall efficiency of DRO with the asymmetric ORS were obtained at beam current $I_a = 153$ mA and were: $N_{max} = 11$ %; $P_{max} = 60$ W. For DRO with symmetric ORS the maximal output power and overall efficiency at beam current $I_a = 150$ mA were: $N_{max} = 9.4$%; $P_{max} = 50$ W.

4. DRO-MODEL WITH DOUBLE GRATING OF HEIGHT $B = 10.0$ MM

For DRO with double grating the significant elongation of H_{10}-mode in elementary waveguides, formed by opposite slots of double grating, is typical. This fact allows using in DRO the broader electron beam, that is especially important at operating in short millimeter waves [2]. On the other hand, selection of double grating parameters, which provides high elongation of H_{10}-mode in its cell, is conducted by narrowing of DRO frequency tuning range and decreasing of ORS Q-factor due to ohmic loss growth in double grating. The problems can be overcome by using in DRO an asymmetric OR with the double grating, shifted to field spot periphery of operating TEM_{00q}-mode.

The verification of asymmetric ORS influence on output characteristics of DRO at double grating height increasing was conducted on DRO-model with double grating of height $b = 10.0$ mm. The used ORS was in semispherical OR form (focusing mirror with curvature $R_{sph} = 50$ mm and aperture ∅55 mm). The other double grating parameters were: grating length – $L = 32$ mm; grating period – $l = 1.00$ mm; slots width $d = 0.50$ mm, and slots depth $h = 2.67$ mm. The estimated frequency of the complete phase matching of double grating with resonant field was: $f_\pi = 31.0$ GHz.

The output power maximum of DRO-model with symmetric ORS at operating on TEM_{004}-mode was observed near $f_\pi = 31.0$ GHz and was $P_{max} = 25$ W, the frequency tuning range at the output power level $P \geq 0.5\ P_{max}$ was $\Delta f/f_\pi = 5.2\%$. When the double grating was shifted on $\xi = 6.0$ mm from ORS longitudinal axis, the oscillation output power maximum increased to $P_{max} = 32$ W, and the frequency tuning range extended to $\Delta f/f_\pi = 6.8\%$ (Fig. 6a). Due to increasing of the interaction space length to $L = 32$ mm $\approx 3.6\ w_{0y}$ the oscillation starting current in DRO with symmetric ORS was only $I_{st} \approx 15$ mA. The oscillation starting current in DRO with asymmetric ORS increased in ~ 2 times and was $I_{st} = (24 \div 33)$ mA at frequencies $f = (29.5\text{-}31.0)$ GHz (Fig. 6b).

A comparison of efficiency on beam-field interaction in DRO-model with the double grating of height $b = 10.0$ mm had been carried out at frequency $f = 31.0$ GHz. It was established, that overall efficiency in DRO with symmetric ORS reached saturation $N_{max} = 7.5$ % at beam current $I_a \geq 100$ mA, and when we used asymmetric ORS the overall efficiency increased without saturation to $N_{max} = 8.8$ % at beam current $I_a = 144$ mA (Fig. 6c).

5. MODE COMPETITION FEATURES IN DRO WITH SYMMETRIC AND ASYMMETRIC ORS

Mode competition, excited by electron beam in ORS, significantly influences on DRO output parameters. Especially strong mode competition phenomenon observed when symmetric ORS was used in DRO. Thus, for DRO with symmetric OR in hemispherical form,

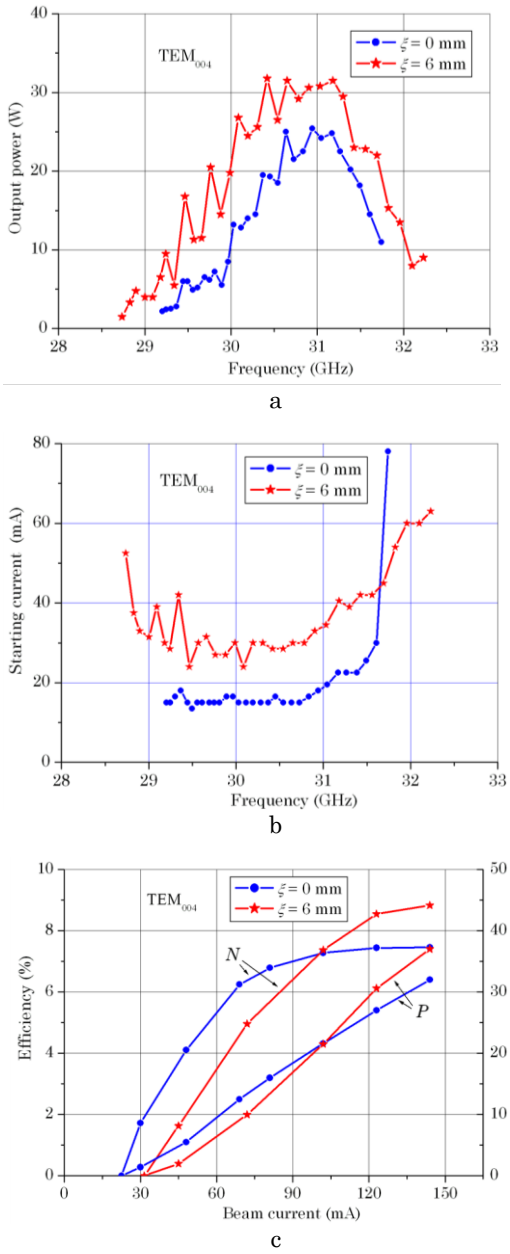

Fig. 6 – The output characteristics of DRO-model with double grating of height $b = 10$ mm at operating on TEM_{004}-mode

the spectrum crashing of resonant modes is observed near semiconfocal geometry at $D \approx 0.5R_{sph}$. In this case, according to the dispersion equation (3) the resonance frequencies placed closely for the fundamental TEM_{00q}-mode and higher transversal $TEM_{mn(q-1)}$-modes with transversal indexes $m + n = 4$.

The usage in DRO an asymmetric ORS allows significant decrease the influence of mode degeneracy near semiconfocal geometry, that was confirmed at experimental investigations of DRO-model with double grating of height $b = 8.0$ mm and interaction space length $L = 25$ mm ($R_{sph} = 50$ mm). So, when DRO operated on TEM_{005}-mode near the semiconfocal geometry ($D \approx 25$ mm), the asymmetric ORS usage allowed significant the frequency tuning range extension without decreasing of DRO output power level. Also, for DRO with symmetric ORS, operated on TEM_{005}-mode, the frequency tuning range was $\Delta f/f_\pi = 3.8$ % due to modes degeneracy. For DRO with asymmetric ORS the frequency tuning range on TEM_{005}-mode extended to $\Delta f/f_\pi = 6.2$ % (Fig. 7).

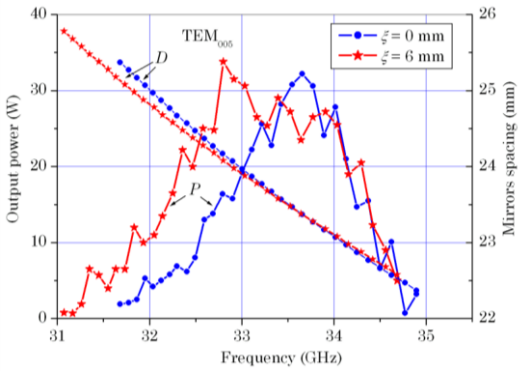

Fig. 7 – The frequency tuning range of DRO with symmetric and asymmetric ORS at operating on TEM_{005}-mode near semiconfocal geometry at $D \approx R_{sph} = 25$ mm

Significant elongation of H_{10}-mode in the elementary waveguides, formed by opposite slots of double grating [3] leads to slope increasing of dispersion curve $D_{00q}(f)$ for fundamental TEM_{00q}-mode, especially at the low-frequency tuning range of DRO at $\lambda \to \lambda_{cr}$. For higher TEM_{mnq}-modes the influence of double grating on resonant field is negligible and their dispersion curves $D_{mnq}(f)$ have a smaller slope and can be defined according to the resonance condition in OR with smooth mirrors (3). The difference in slope of dispersion curves $D(f)$ for operating TEM_{00q}-mode and higher TEM_{mnq}-modes may leads to mode degeneracy and their competition at low-frequencies of DRO tuning range [4]. Besides, owing to small asymmetry in DRO-model, caused by mirrors distortion, a competition of operating TEM_{00q}-mode occurs both with even and odd higher TEM_{mnq}-modes.

For example, consider the modes degeneracy features in DRO-model with symmetric and asymmetric ORS ($R_{sph} = 50$ mm; $b = 8.0$ mm; $f_\pi = 33.7$ GHz) at operating on TEM_{004}-mode. The output characteristics of DRO-operating on TEM_{004}-mode are shown on Fig. 3. The experimental dispersion curves $D_{004}(f)$ for DRO-operating on TEM_{004}-mode with symmetric and asymmetric ORS are shown on Fig. 8. Here the dispersion curves for nearest resonant modes in hemispherical OR with smooth mirrors are shown by solid lines: TEM_{403}-mode (Fig. 8, curve 1); TEM_{004}-mode (Fig. 8, curve 2) and TEM_{503}-mode (Fig. 8, curve 3).

The competition of operating TEM_{004}-mode with the higher ones should be expected in DRO near the intersection points of the dispersion curves. Thus, for DRO-model with symmetric ORS the intersection point of the dispersion curves for the TEM_{004} mode and higher TEM_{503}-mode is on frequency $f = 31.6$ GHz (Fig. 8, point A). In DRO-model with asymmetric ORS the influence of double grating on resonant field decreases, and dispersion curve slope for operating TEM_{004}-mode is diminished. As a result, the intersection point of dispersion curves for TEM_{004}- and TEM_{503}-modes shifts to the low-frequency region (Fig. 8, point B), and this fact leads to extension of DRO frequency tuning range on TEM_{004}-mode without mode competition (Fig. 3a).

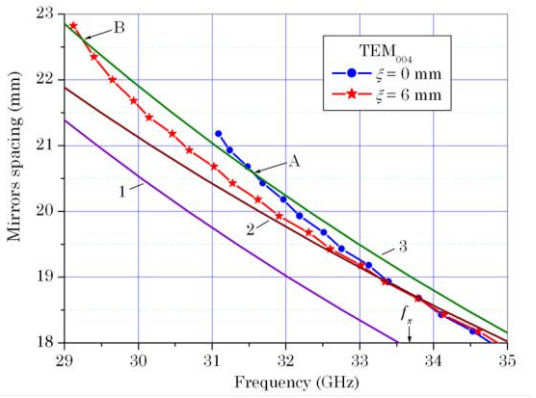

Fig. 8 – Degeneracy mode features in DRO with symmetric and asymmetric ORS (dispersion curves $D_{mnq}(f)$ for the resonant modes in OR with smooth mirrors are shown by solid lines: 1 – TEM_{403}-mode; 2 – TEM_{004}-mode; 3 – TEM_{503}-mode)

The shown above cases of modes competition influence on DRO output characteristics by means of energy exchange between modes at resonant field. But DRO operating can be affected by the ORS modes, which don't interact through resonant field, but directly interact with electron beam. We'll call this case, as mode competition on beam accelerating voltage. For DRO with double grating, operated on TEM_{00q}-mode, the potential competitor on accelerating voltage is the TEM_{01q}-mode with two antiphase field spots along interaction space [5, 6]. The suppression of DRO excitation on TEM_{01q}-mode is realized by reduction of ORS mirrors aperture along *OY* axis (Fig. 1) and truncation of interaction space length. A more radical way is the DRO-operating only on TEM_{01q}-mode, using the shifting of grating slots periodicity in the center of interaction space [7].

For DRO with asymmetric ORS, operated on TEM_{00q}-mode, except the TEM_{01q}-mode a potential competitor on accelerating voltage is the TEM_{10q}-mode with two field spots along *OX* axis (Fig. 9a). The DRO excitation on TEM_{10q}-mode isn't observed when we use the symmetric ORS, due to symmetric location of double grating in anti-phase field spots of this mode. In DRO with asymmetric ORS the double grating is placed on flat mirror near the field maximum of TEM_{10q}-mode (Fig. 9a), that promotes the effective energy exchange between electron beam and resonant field of TEM_{10q}-mode. The resonant frequencies of these modes at fixed distance between ORS mirrors satisfy the inequality $f_{10q} > f_{00q}$, and DRO electronic tuning zone of TEM_{10q}-mode is placed above on DRO electronic tuning zone of TEM_{00q}-mode (Fig. 9b). This leads to hard condition of DRO-operating on TEM_{00q} mode near the output power maximum and to failure of oscillations at the increase of beam current value.

The experimental studies of the competition features by accelerating voltage between TEM_{004} and TEM_{104}-modes had been carried out in DRO-model with asymmetric ORS and double grating of height $b = 10.0$ mm. The output characteristics of such DRO at the tuning on TEM_{004}-mode are shown on Fig. 6. The resonant frequencies separation of TEM_{104} and TEM_{004}-modes at the equal distance *D* between ORS mirrors was $f_{104} - f_{004} \approx 1{,}3$ GHz throughout the all tuning range (Fig. 10a), i.e. the direct mode competition on resonant field wasn't observed. The excitation of oscillation in DRO-model on TEM_{104}-mode was observed at starting current, comparable to the oscillation starting current on TEM_{004}-mode. At the DRO-operating on TEM_{104}-mode the resonant increase of starting current was observed near the frequency $f_{104} \approx f_\pi = 31.0$ GHz at $D = 21.5$ mm (Fig. 10a), caused by the degeneracy of the TEM_{104} and TEM_{014} modes in ORS at complete phase matching of double grating with resonant field.

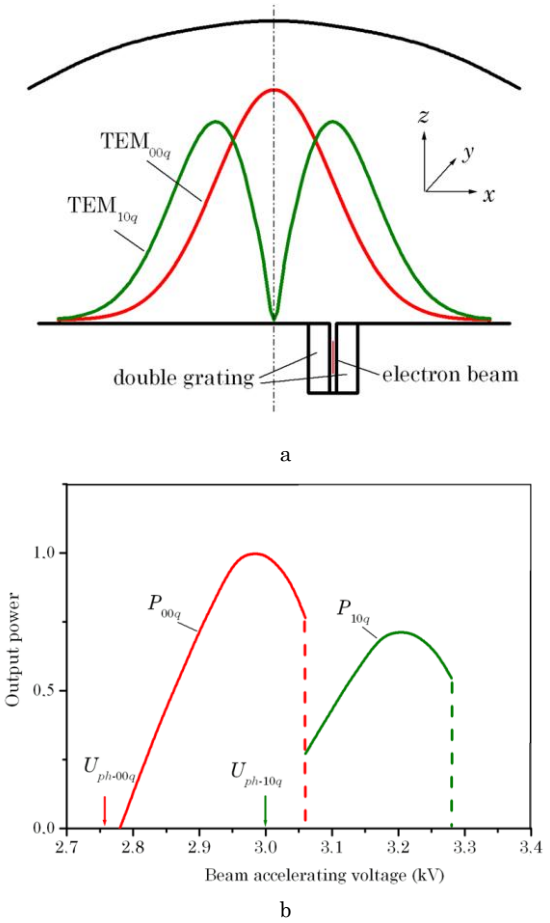

Fig. 9 – The sketch of field structure of TEM_{00q} and TEM_{10q}-modes on the flat mirror of asymmetric ORS (a) and the relative position of DRO electronic tuning zones for TEM_{00q} and TEM_{10q}-modes (b)

In the experiment, at the same distance *D* between ORS mirrors we registered the value of accelerating voltage at the beginning (U_{min}) and at the end of electronic tuning zone (U_{max}) for DRO-operation on TEM_{004} and TEM_{104}-modes.

The synchronous accelerating voltage U_{ph}, which satisfies the velocity synchronism between electron beam and 1-st space harmonic of doble grating periodic field for TEM_{004} and TEM_{104}-modes was obtained according to (1) on measured in experiment resonant frequencies of modes at the given distance *D* between mirrors of ORS.

The beginning of DRO electronic tuning zone on TEM_{004}-mode ($U_{min\text{-}004}$) practically coincided with synchronous accelerating voltage for TEM_{004}-mode ($U_{ph\text{-}004}$) (Fig. 10b). The end of DRO electronic tuning zone on

TEM$_{004}$-mode ($U_{max\text{-}004}$) exceeded the synchronous voltage for TEM$_{104}$-mode ($U_{ph\text{-}104}$) practically throughout the frequency tuning range of DRO (Fig. 10b). Only on the upper frequency tuning area at the distance between mirrors $D = (19.5 \div 19.9)$ mm, where the DRO operated at low level of output power, the overlapping of electronic tuning zone for TEM$_{004}$ and TEM$_{104}$-modes wasn't observed.

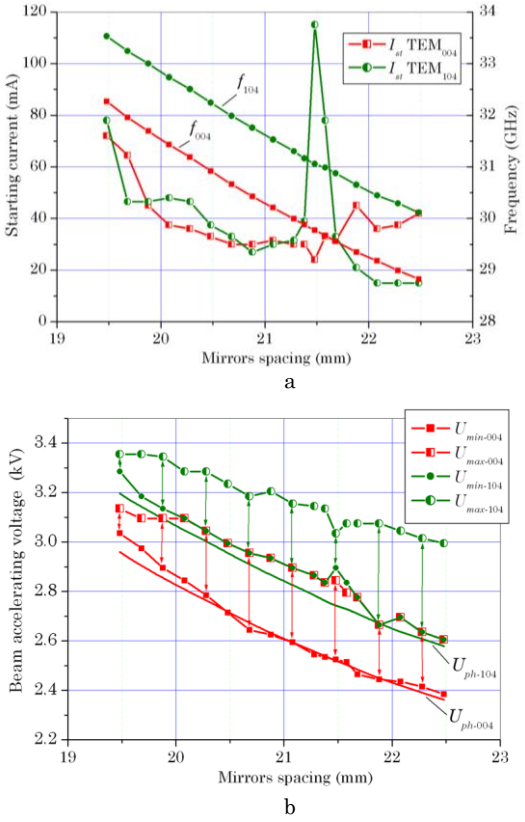

Fig. 10 – The competition by accelerating voltage for TEM$_{004}$ and TEM$_{104}$-modes in DRO with asymmetric ORS: a comparison of oscillation starting current for DRO-operating on TEM$_{004}$ and TEM$_{104}$-mode (a) and overlapping of electronic tuning zones for DRO-operating on TEM$_{004}$ and TEM$_{104}$-mode at the same distance D between ORS mirrors (b)

The result of considered above modes competition on accelerating voltage is a hard condition of DRO-operating on TEM$_{004}$-mode near output power maximum. The suppression of DRO excitation on TEM$_{104}$-mode is realized by reduction of ORS mirrors aperture along OX axis (Fig. 1).

The next case of mode competition on accelerating voltage in DRO is the interaction of electron beam with slow backward wave in periodic structure (so called the BWO-mode of operation) [8-10]. The starting current growth in DRO with asymmetric ORS can lead to hard competition of DRO-mode and BWO-mode. To suppress the excitation of DRO-model on BWO-mode it is necessary to reduce the length of periodic structure, or to use the periodicity failure in the centre of grating.

6. CONCLUSION

1. The hot tests of DRO-model confirm the advantages of using asymmetric ORS for frequency tuning range extension. Thus, in DRO-model with double grating of height $b = 8.0$ mm the frequency tuning range extended in 1.5 times and for the output power level $P \geq 0.5\ P_{max}$ was $\Delta f/f_{\pi} = 9.4$ % at $P_{max} = 35$ W. The usage of asymmetric ORS for DRO-model with double grating of height $b = 10.0$ mm allowed to extend the frequency tuning range in 1.3 times: $\Delta f/f_{\pi} = 6.8$ % at $P_{max} = 32$ W.

2. The displacement of double grating to field spot periphery in asymmetric ORS led to increasing of oscillation starting current in 1.5-2 times, but also reduced the influence of electron beam regrouping on output power level of DRO at beam current increasing. Also, DRO with asymmetric ORS had the advantage in output power and overall efficiency at beam currents $I_a > 90$ mA. Thus, at beam current $I_a = 150$ mA the overall efficiency in DRO with asymmetric ORS was $N = 11$ % and maximum output power level was $P_{max} = 60$ W, but when we used symmetric ORS in DRO at the same beam current the output parameters of DRO were: $N = 9.4$ % and $P_{max} = 50$ W.

3. It is shown, that in DRO with asymmetric ORS it is possible to avoid traditional mode degeneracy near semiconfocal ORS-geometry. Also, in such DRO it is possible to shift zone of modes competition for operating TEM$_{00q}$-mode and higher TEM$_{mn(q-1)}$ modes in region of lower frequencies, and it contributes to extend the DRO single-mode tuning range.

4. The disadvantage of DRO with asymmetric ORS is the presence of additional competition by accelerating voltage between operating TEM$_{00q}$-mode and TEM$_{10q}$-mode, one of two field spots of which falls on the double grating, shifted from the longitudinal axis of ORS.

Генератор дифракційного випромінювання з асиметричною відкритою резонансною системою. Частина 2. Результати "гарячих" досліджень генератора дифракційного випромінювання

В.С. Мірошниченко, Є.О. Ковальов

Інститут радіофізики та електроніки ім. О.Я. Усикова НАН України, вул. Академіка Проскури, 12, 61085 Харків, Україна

Представлені результати "гарячих" досліджень генератора дифракційного випромінювання з асиметричною відкритою резонансною системою, в якій періодична структура зміщена на периферію плями поля робочої TEM_{00q}-моди. Показано, що розміщення періодичної структури у вигляді здвоєної гребінки на периферії плями поля TEM_{00q}-моди дає можливість розширити одномодовий діапазон перебудови по частоті та підвищити загальний ККД генератора дифракційного випромінювання. Розглянуто особливості конкуренції мод в генераторі дифракційного випромінювання зі здвоєною гребінкою та асиметричною відкритою резонансною системою.. Дослідження виконані у 8-мм діапазоні довжин хвиль.

Ключові слова: Генератор дифракційного випромінювання, Відкрита резонансна система Періодична структура, Здвоєна гребінка, Міліметрові хвилі.

Генератор дифракционного излучения с асимметричной открытой резонансной системой. Часть 2. Результаты "горячих" исследований генератора дифракционного излучения

В.С. Мирошниченко, Е.А. Ковалев

Институт радиофизики и электроники им. А.Я. Усикова НАН Украины, ул. Академика Проскуры, 12, 61085 Харьков, Украина

Представлены результаты "горячих" исследований генератора дифракционного излучения с асимметричной открытой резонансной системой, в которой периодическая структура смещена на периферию пятна поля рабочей TEM_{00q}-моды. Показано, что размещение периодической структуры в виде сдвоенной гребенки на периферии пятна поля TEM_{00q}-моды дает возможность расширить одномодовый диапазон перестройки по частоте и улучшить общий КПД генератора дифракционного излучения. Рассмотрены особенности конкуренции мод в генераторе дифракционного излучения со сдвоенной гребенкой и асимметричной открытой резонансной системой. Исследования выполнены в 8-мм диапазоне длин волн.

Ключевые слова: Генератор дифракционного излучения, Открытая резонансная система, Периодическая структура, Сдвоенная гребенка, Миллиметровые волны.

REFERENCES

1. *Diffraction radiation generators* (Ed. by V.P. Shestopalov) (Kiev: Naukova dumka: 1991), [in Russian].
2. V.K. Korneenkov, V.S. Miroshnichenko, B.K. Skrynnik,. *Telecommunicat. Radio Eng.* **51** No 6-7, 144 (1997).
3. V.S. Miroshnichenko, I.O. Kovalov, *J. Nano- Electron. Phys.* 8 No 2, 02033 (2016).
4. V.S. Miroshnichenko, *Telecommunicat. Radio Eng.* **68** No 3, 231 (2009).
5. Yu.I. Evdokimenko, K.A. Lukin, I.D. Revin, B.K. Skrynnik, *Zh. Tekh. Fiz.* **52** No 3, 525 (1982) [in Russian].
6. A.N. Solovyov, M.B. Tseytlin, *Radiotekh. Electron.* **27** No 2, 368 (1982) [in Russian].
7. V.S. Miroshnichenko, E.B. Senkevich, A.G. Pivovarova, D.V. Yudintsev, *Radiophys. Quantum Electron.* **53** No 3, 182 (2010).
8. I.M. Balaklitsky, V.G. Kurin, B.K. Skrynnik, *Ukr. Phys. J.* **15** No 5, 717 (1970), [in Russian].
9. F.S. Rusin, V.P. Kostromin, *Radiotekh. Electron.* **30** No 5, 994 (1985) [in Russian].
10. M.Yu. Demchenko, V.K. Korneenkov, V.S. Miroshnichenko, B.K. Skrynnik, *Radiofizika i electronika* **4** No 2, 99 (1999) [in Russian].